ORIGINAL ARTICLE

Enhancement of T Follicular Helper Cell-Mediated Humoral Immunity Reponses During Development of Experimental Autoimmune Myasthenia Gravis

Ying-Zhe Cui[1] · Si-Ying Qu[1] · Lu-Lu Chang[1] · Jia-Rui Zhao[1] · Lili Mu[1] ·
Bo Sun[1] · Hu-Lun Li[1] · Tong-Shuai Zhang[1] · Guang-You Wang[1] · Qing-Fei Kong[1]

Abstract Myasthenia gravis (MG) is a prototypical antibody-mediated neurological autoimmune disease with the involvement of humoral immune responses in its pathogenesis. T follicular helper (Tfh) cells have been implicated in many autoimmune diseases. However, whether and how Tfh cells are involved in MG remain unclear. Here, we established and studied a widely-used and approved animal model of human MG, the rat model with acetylcholine receptor alpha (AChRα) subunit (R-AChR$_{97-116}$)-induced experimental autoimmune myasthenia gravis (EAMG). This model presented mild body-weight loss 10 days after the first immunization (representing the early stage of disease) and more obvious clinical manifestations and body-weight loss 7 days after the second immunization (representing the late stage of disease). AChR-specific pre-Tfh cells and mature Tfh cells were detected in these two stages, respectively. In cocultures of Tfh cells and B cells, the number of IgG2b-secreting B cells and the level of anti-AChR antibodies in the supernatant were higher in the cultures containing EAMG-derived Tfh cells. In immunohistochemistry and immunofluorescence assays, a substantial number of CD4$^+$/Bcl-6$^+$ T cells and a greater number of larger germinal centers were observed in lymph node tissues resected from EAMG rats. Based on these results, we hypothesize that an AChR-specific Tfh cell-mediated humoral immune response contributes to the development of EAMG.

Keywords Follicular helper T cells · Experimental autoimmune myasthenia gravis · Acetylcholine receptor · Germinal center

Introduction

Myasthenia gravis (MG) is an autoimmune disease characterized by pathological changes at the postsynaptic membrane of neuromuscular junctions. These changes are mediated by antibodies that bind to self-acetylcholine receptors (AChRs) or to functionally-related molecules [1, 2]. The subsequent loss of AChRs initiates muscle contractions and induces skeletal muscle weakness to cause fatigue [3]. In the clinic, autoimmune antibodies have been identified in the serum of MG patients and a therapeutic effect has been reported in MG patients following CD20-mediated B cell depletion. Therefore, MG is regarded as a B cell-mediated autoimmune disease.

When B cells encounter an antigen, they become activated and migrate into lymphoid follicle areas to form germinal centers (GCs) and differentiate into plasma cells that produce autoantibodies [4, 5]. At each of these steps, interactions between T cells and B cells are required. Furthermore, these interactions are mediated by cytokines, chemokines, and T follicular helper (Tfh) cells [6, 7]. Tfh cells are a specialized subset of CD4$^+$ helper T cells which prime B cells located in GCs and subsequently reside in B cell-enriched GCs to support B cell differentiation and antibody production [8, 9]. Tfh cells express high levels of C-X-C chemokine receptor type 4 (CXCR5), CD40 ligand,

Ying-Zhe Cui and Si-Ying Qu have contributed equally to this work.

✉ Guang-You Wang
guangyouwang@163.com

✉ Qing-Fei Kong
kqfangel@hrbmu.edu.cn

[1] Department of Neurobiology, Heilongjiang Provincial Key Laboratory of Neurobiology, Harbin Medical University, Harbin 150081, China

interleukin (IL)-21, and transcriptional factor B cell lymphoma 6 (Bcl-6). Bcl-6 is essential for Tfh cell differentiation and for the functions of these cells. In addition, high levels of expression of the cell surface molecules inducible T cell co-stimulator (ICOS) and programmed cell death protein 1 (PD-1) are necessary for the differentiation of Tfh cells and their functions [10, 11]. For example, both ICOS and PD-1 provide specific auxiliary signals for the migration and location of cognate B cells in secondary lymphoid tissue follicles and GCs.

Due to the essential roles of Tfh cells and the molecules they express in humoral immunity, overabundance or dysregulation of Tfh cells can facilitate the production of autoantibodies. The production of autoantibodies is a key aspect of various human diseases, including hyper-IgM syndrome [12], systemic lupus erythematosus (SLE) [13], rheumatoid arthritis [14], and neuroautoimmune diseases [15, 16]. In MG patients, a higher frequency of Tfh cells in the thymus and a greater number of $CXCR5^+ CD4^+$ T cells in the periphery have been reported [17–19]. Thus, these findings suggest that Tfh cells contribute to the pathogenesis of MG. However, the exact pathogenic mechanisms involving Tfh cells in MG have not been clearly elucidated. Therefore, in this study, we examined the lymph node tissues of a widely-used and approved animal model of human MG, the AChRα subunit (R-AChR$_{97-116}$)-induced experimental autoimmune myasthenia gravis (EAMG) rat model [20], in which $CD4^+$ T cells contribute to the pathogenesis of EAMG by promoting the production of anti-AChR antibodies by B cells [21, 22].

Materials and Methods

Animals

Eight-week-old female Lewis rats (weighing 140 g–160 g) were purchased from Vital River Laboratory Animal Co. Ltd. (Beijing, China) and maintained according to the principles outlined in the Harbin Medical University's Guide for the Care and Use of Laboratory Animals published by the China National Institute of Health. The studies performed were also approved by the Institutional Animal Care and Use Committee of Harbin Medical University.

Clinical Evaluation of EAMG

Specific peptides corresponding to the rat AChRα subunit (R-AChR$_{97-116}$) described previously [23] were synthesized by AC Scientific, Inc. (Xi'an, China). These peptides were determined to be 95% pure by HPLC analysis. EAMG was induced as described previously [24]. Briefly,

the rats were anesthetized with diethyl ether and immunized with 200 μL of inoculums containing 50 μg R-AChR$_{97-116}$ peptide and 1 mg *Mycobacterium tuberculosis* strain H37RA (Difco, Detroit, MI) emulsified in incomplete Freund's adjuvant (IFA, Sigma Aldrich, St Louis, MO) at the base of the tail on day 0. Thirty days later, the rats received a second immunization with the same dose of R$_{97-116}$ peptide emulsified in IFA without *M. tuberculosis*. In parallel, rats in the control group only received complete Freund's adjuvant (CFA) that contained the same dose of IFA, *M. tuberculosis*, and phosphate-buffered saline (PBS) at their first immunization, and received only IFA at their second immunization. Disease severity was evaluated from the first immunization based on assessments of muscular weakness and body weight loss in a blinded manner. Fatigue was assessed after a 30-s exercise regimen of repetitive paw grips on the cage grid. Clinical signs were observed every second day until the time of sacrifice and were scored as previously described [20, 25]: 0, no disease; 1, mildly decreased activity and weak grip or cry, more evident at the end of testing; 2, obvious clinical signs before exercise (i.e., tremors, head down, hunched posture, weak grip); 3, severe clinical signs already present before exercise, no grip, moribund; 4, dead. Scores of 0.5, 1.5, 2.5, or 3.5 were assigned to rats exhibiting intermediate signs. Mean scores were reported for each treatment group at each time point. Animal model induction rate was greater than 85%.

Enzyme-Linked Immunosorbent Assay (ELISA)

Serum/supernatant anti-AChRα subunit (R-AChR$_{97-116}$) antibody was detected by ELISA. Blood samples were collected from the thigh vein on day 0 prior to the first immunization, and subsequently every six days until the time of sacrifice. ELISA plates (Corning Costar 96-well plates, eBioscience, San Diego, CA) were pre-coated with affinity-purified R-AChR$_{97-116}$ peptide (2 μg/mL) in 100 μL of 0.1 mol/L coating buffer (pH 9.6) overnight at 4°C. After the plates were washed with 0.05% PBS/Tween 20 (PBS-T), they were blocked with 10% fetal calf serum at room temperature (RT). After 2 h, 100 μL serum samples at dilutions of 1:100, 1:5000, and 1:10000, or supernatants without dilution, were added into each well and incubated at 37°C for 2 h. After 4 washes with PBS-T, rabbit anti-rat IgG antibody diluted 1:2000 in blocking buffer was added to each well. After 2 h incubation at RT, horseradish peroxidase (HRP)-conjugated goat anti-rabbit IgG (1:5000 dilution, 100 μL) was added to each well and incubated at 37°C for 1 h. After the plates were washed with PBS-T, 100 μL TMB substrate solution (Biolegend, San Diego, CA) was added to each well. After 15 min at RT in the dark, the reactions were stopped by addition of 50 μL of 2

mol/L H_2SO_4. Absorbance was read at 450 nm with a Bio-Rad microplate reader (Bio-Rad Laboratories, Inc. Hercules, CA) and optical density values are presented as mean ± standard deviation (SD).

Tissue Sampling and Immunostaining

Rats were deeply anesthetized prior to tissue resection, after which tissues were immediately cryoprotected in Tissue-Tek OCT Compound (Sakura, Japan). Specimens were sectioned at various thicknesses. Rat lymph nodes for staining with peanut agglutinin (PNA) or Bcl-6 antibodies were cut at 7 μm, subsequently quenched with 0.3% H_2O_2 in methanol for 15 min, and then blocked in 5% normal horse serum for 30 min. The sections were then incubated with PNA-biotin (1:500 dilution in PBS; Abcam, Cambridge, MA) or rabbit anti-rat-Bcl-6 secondary antibodies (diluted 1:100 in PBS; Abcam) overnight at RT. After a wash step with PBS, the sections were incubated with streptavidin-conjugated HRP for 2 h. The substrate-chromogen, DAB, was added to visualize PNA-positive cells and Bcl-6-positive cells. Finally, the sections were counterstained with hematoxylin for 1 min.

For immunofluorescence analysis, 10 μm-thick frozen sections were prepared and air-dried for alpha-bungarotoxin (α-BTX) staining. After a fixation step in cold acetone for 10 min, sections were blocked in 5% normal horse serum and then stained with tetramethylrhodamine-labeled α-BTX (1:500 diluted in 5% horse serum) overnight at 4°C. To detect Tfh cells, 7-μm frozen sections of lymph tissues were double stained with Bcl-6 and CD4. The staining protocol was similar to that for α-BTX staining, except that the sections were incubated with rabbit anti-rat-Bcl-6 (diluted 1:100 in PBS; Abcam) and mouse anti-rat-CD4 antibodies (diluted 1:500; Abcam) overnight at 4°C. In addition, anti-mouse FITC IgG (ZSGB-BIO, Beijing, China) and anti-rabbit Alexa 555 IgG (Invitrogen, CA) secondary antibodies were incubated with the sections for an additional 2 h. Finally, the sections were observed under an LSM700 confocal microscope (Carl Zeiss, Germany) and imaged under the same conditions. Quantitative immunofluorescence analysis was performed as previously described with minor modifications [23]. Dense AChR clusters were labeled red and Tfh cells were defined as $CD4^+$-Bcl-6^+ cells in lymph nodes. The sections from all of the groups were stained and processed in parallel to avoid inter-assay variations.

Flow Cytometry

Propidium Iodide (PI, Biolegend, San Diego, CA) and 5(6)-Carboxyfluorescein diacetate succinimidyl ester (CFSE, Biolegend) staining was performed following the manufacturer's instructions to mark PI-negative CFSE-positive live cells. Nuclear transcription factors and cell surface markers were detected by flow cytometry as described previously [26]. Briefly, cells were first incubated with anti-rat-CD4-FITC, CD4-PERCP, CD45R-PE (Biolegend), PNA-FITC, CD4-APC, ICOS-PE, CXCR5-PERCP, and CD86 PE (Biolegend) antibodies for 30 min at 4°C. Intranuclear staining was performed with Bcl-6-APC and IgG2b-FITC antibodies (Biolegend) after cells were fixed and permeabilized. Tfh cells were stained with FITC-anti-rat-CD4/APC-anti-rat-Bcl-6 ($CD4+Bcl6+$) or FITC-anti-rat-CD4/PE-anti-rat-ICOS/Percp-anti-rat-CXCR5 ($CD4+CXCR5+ICOS++$) combinations of antibodies.

Mononuclear cells were obtained from the inguinal, popliteal, para-aortic, and axillary lymph nodes of immunized animals. These cells were subsequently stimulated with 10 μg/mL R-$AChR_{97-116}$ in RPMI 1640 medium (Sigma-Aldrich) supplemented with 1% sodium pyruvate, 10% heat-inactivated fetal bovine serum, 1% non-essential amino-acids, 1% L-glutamine (Sigma-Aldrich), 1% penicillin-streptomycin (Gibco, Paisley, UK), and 2-mercaptoethanol (2×10^{-5} mol/L, Amresco, Solon, OH) for 72 h and then stained as described above. Samples were analyzed within 24 h of staining using a BD FACScan (BD Biosciences, San Jose, CA) and analyzed with Cell Quest software (BD Biosciences). Isotype-matched, FITC-, Percp-, APC-, and PE-conjugated monoclonal antibodies of irrelevant specificity were used as negative controls.

Isolation of $CD4^+$ T cells/$CD45R^+$ B cells and RT-PCR

Axillary, inguinal, popliteal, and para-aortic lymph nodes were dissected seven days after the first immunization. Mononuclear cells were harvested by passing cell suspensions through a 40-μm nylon mesh. $CD4^+$ T cells and $CD45R^+$ B cells were subsequently isolated by negative selection with a MagCellect Rat $CD4^+$ T Cell Isolation Kit or a Magcellect Rat B cell Isolation Kit (R&D Systems, Inc. Minneapolis, MN) according to the manufacturer's instructions.

Total RNA was isolated from enriched $CD4^+$ T cells with TRIzol reagent (Invitrogen) according to the manufacturer's instructions. Complementary DNA was synthesized for each 1 μg total RNA sample with an RT-PCR kit (TaKaRa, Japan) and a 7500 real-time PCR system was used to perform semi-quantitative amplification. β-actin was used as an internal control. The primers used (listed $5' \rightarrow 3'$) were: Bcl-6 forward: ATCGAGGTCGT-GAGGTTGTG, reverse: TCGGATAAGAGGCTGGTGG; β-actin forward: AGGAGTACGATGAGTCCGGC, reverse: AAGAAAGGGTGTAAAACGCAGC.
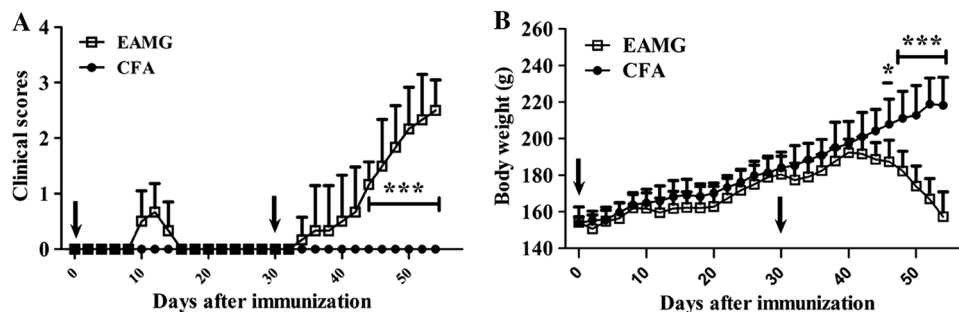
Fig. 1 Clinical scores and body weights. Clinical scores (**A**) and body weights (**B**) were recorded for both CFA and EAMG rats every other day after the first immunization. Mild clinical signs occurred ~10 days after the first immunization. Clinical manifestations of EAMG then gradually became evident 7 days after the second immunization. Arrows indicate immunization time-points. In contrast, rats in the CFA group showed no clinical signs of EAMG or any abnormal weight loss. Data are from two independent experiments with 6 rats per condition per experiment (*$P < 0.05$, ***$P < 0.001$).

Co-culture Assays with Tfh Cells and B Cells

To enrich Tfh cells *in vitro*, CD4$^+$ T cells were isolated from both CFA and EAMG rats. T cells were plated in 48-well plates (500 μL at 1×10^6/mL) and stimulated with 10 μg/mL AChR peptide at 37°C. After 24 h, 200 μL of freshly-isolated CD45R$^+$ B cells (1×10^7/mL) from EAMG rats were added to each well for co-culture for another 24 h. The B cells and supernatant fractions from each well were analyzed by flow cytometry with staining to detect antibody secretion with anti-rat-B220-PE and IgG2b-FITC (Biolegend) antibodies, as well as by ELISA as described above.
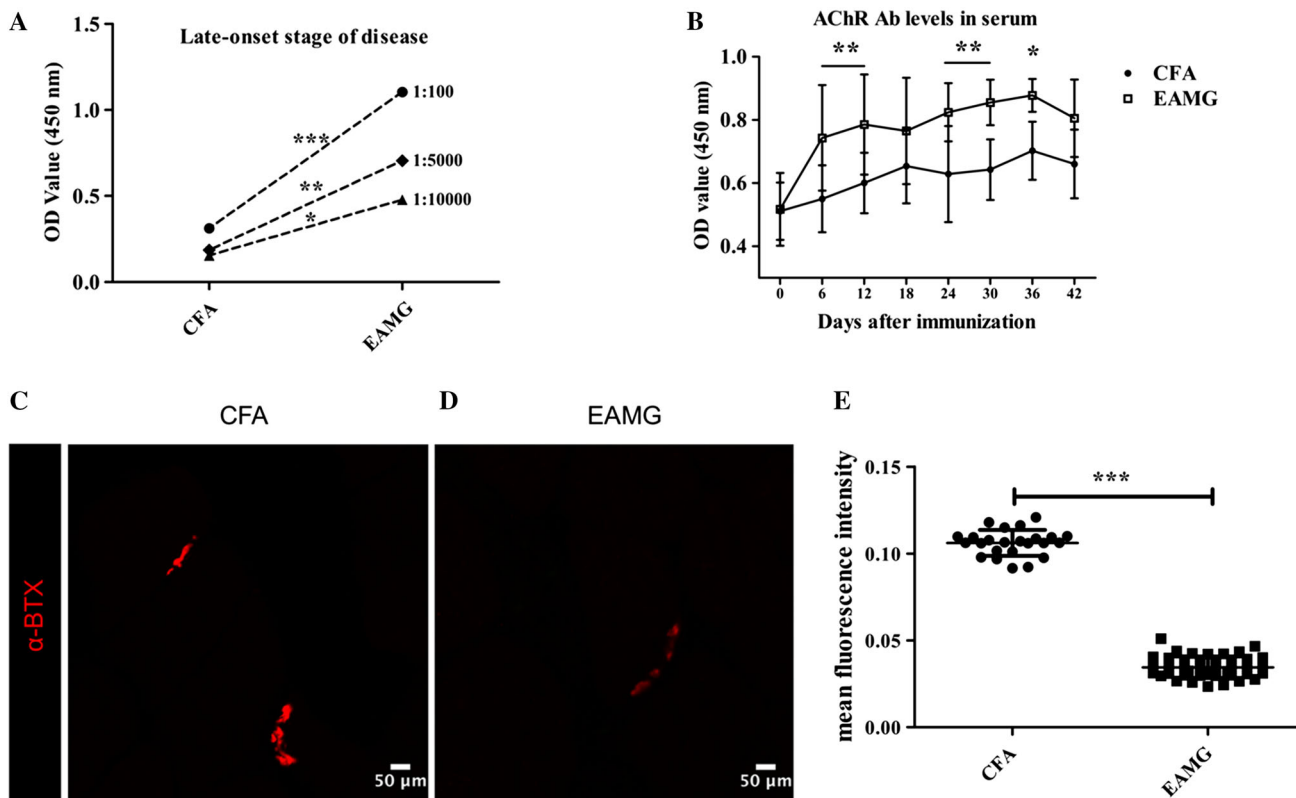

Fig. 2 Elevated levels of auto-AChR antibodies in serum and a reduction in AChRs in muscles. **A** ELISAs were used to detect anti-AChR IgG titers on day 45 in samples diluted 1:100, 1:5000, and 1:10000 from the EAMG and CFA groups ($n = 3$ rats/group). **B** Anti-AChR antibody levels in serum samples collected from the two groups every 6 days after the first immunization ($n = 6$ rats/group) assessed by ELISA. **C**, **D** Forelimb muscle from EAMG (**D**) and CFA (**C**) rats stained with α-BTX as a marker of AChRs. Scale bars, 50 μm; $n = 4$ rats/group. **E** Fluorescence intensity values (mean ± SD; *$P < 0.05$, **$P < 0.01$, ***$P < 0.001$).

Statistical Analysis

Graphpad Prism 5 software (GraphPad, San Diego, CA) was used for statistical analyses. Data are expressed as the mean $\pm$ SD. An unpaired Student's *t*-test was used to compare numerical data between two groups, while one-way analysis of variance (ANOVA) was used to compare data from multiple groups. The statistical differences between CFA and EAMG in clinical score, body weight, and anti-AChR antibody level were analyzed with two-way repeated measures ANOVA followed by Bonferroni's *post-hoc* test. A two-tailed *P* value of < 0.05 was considered statistically significant.

Results

Establishment of the EAMG rat model

Clinical scores and body weight of the AChR-immunized rats were evaluated every other day after the initial immunization (Fig. 1). Mild body weight loss (representing mild signs) occurred ~ 10 days after the first immunization (representing the early stage of disease) (Fig. 1A, B). More typical clinical manifestations and body weight loss were gradually evident 7 days after the second immunization (representing the late stage of disease) (Fig. 1A, B). The anti-AChR IgG titers (Fig. 2A) in serum samples collected from the EAMG rats were significantly higher than those from the CFA rats, independent of the stage of disease or the time of sample collection (samples were collected every 6 days after the primary immunization) (Fig. 2B). However, no further elevation in titer levels occurred after day 36 post-immunization.

Forelimb muscle tissue from EAMG and control rats was collected on day 37. This tissue was stained for α-BTX, a marker of AChRs. The AChR clusters in the EAMG group were weaker and elongated (Fig. 2D) compared to those in the CFA group (Fig. 2C, E), implying a marked reduction of AChRs in EAMG rat muscle. Thus, the appearance of MG-like clinical signs, elevated anti-AChR IgG levels, and a decrease in the number of AChRs in the AChR-immunized rats indicated that the rat model of EAMG was successfully established.

Pre-Tfh and Tfh Cells Contribute to the Development of EAMG

To determine whether Tfh cells participate in the progression of EAMG, $CD4^+CXCR5^+$ (Fig. 3C, D) and
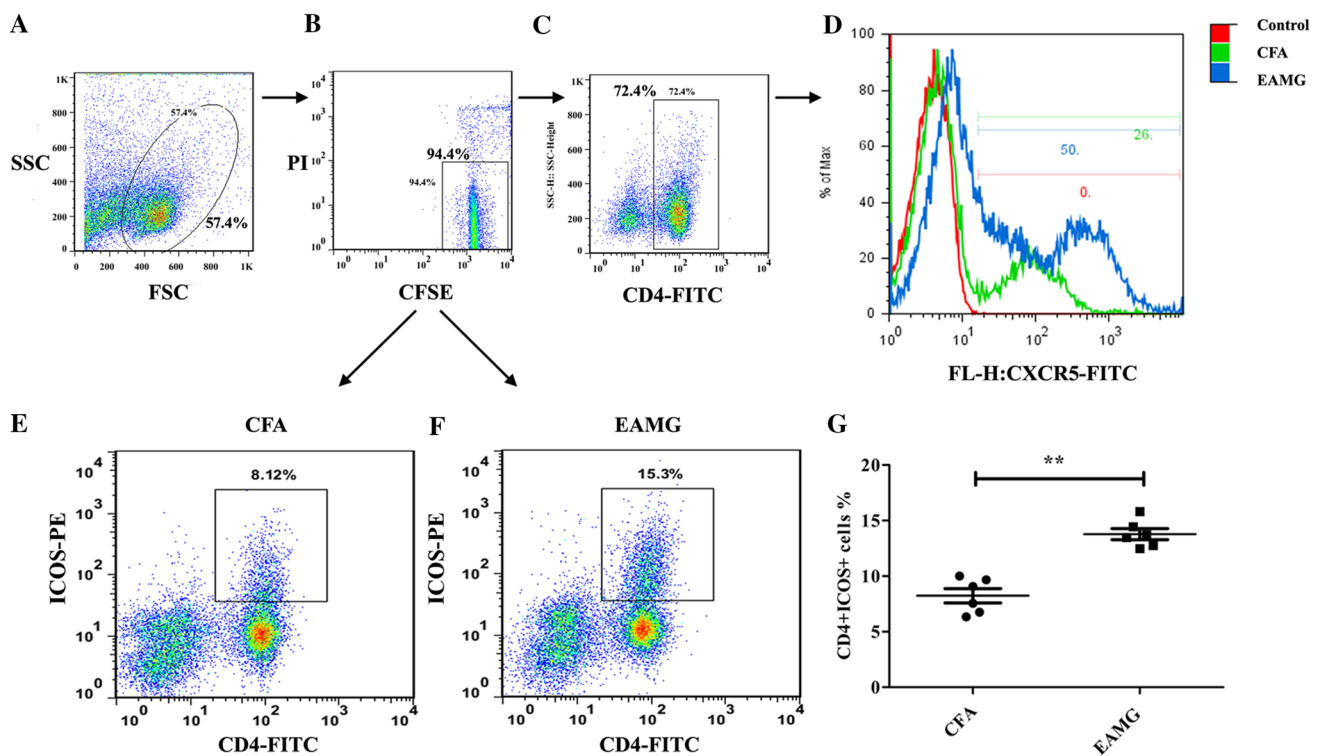

Fig. 3 Pre-Tfh cells among lymphoid cells. **A–F** Cells were gated according to forward scatter/side scatter (FSC/SSC) (**A**) and then by PI and CFSE (**B**). Only PI-negative and CFSE-positive cells (i.e., live cells) were gated and then analyzed for pre-Tfh cells, including $CD4^+CXCR5^+$ (**C**, **D**) and $CD4^+ICOS^+$ T cells (**E**, **F**). (**G**) Percentage of $CD4^+ICOS^+$ T cells in each group (mean $\pm$ SD; data from three independent experiments with 6 rats per condition per experiment; **$P < 0.01$).

CD4$^+$ICOS$^+$ cells (Fig. 3E–G) were detected with flow cytometry. Initially, PI and CFSE staining were performed to ensure that only live cells were analyzed (i.e., PI-negative and CFSE-positive cells) (Fig. 3A, B). Compared with cells isolated from the CFA group, there was a marked increase in the percentages of CD4$^+$CXCR5$^+$ (Fig. 3C, D) and CD4$^+$ICOS$^+$ (Fig. 3E–G) cells, which are regarded as pre-Tfh cells, in the EAMG group. In contrast, very few mature Tfh cells were detected (data not shown). At the late stage of disease, a greater number of CD4$^+$Bcl-6$^+$ cells (Fig. 4A–C) and CD4$^+$CXCR5$^+$ICOS^{++} (Fig. 4D–F) Tfh cells were isolated from the EAMG rats compared with the control rats. Moreover, these data corresponded with the clinical observations of late EAMG. Taken together, these results indicated that AChR-specific pre-Tfh cells and mature Tfh cells participate in the development of EAMG.

Elevated Anti-AChR IgG Levels in Co-cultures of B Cells and Tfh Cells

Currently, Tfh cells are considered to be the most important helper T cell population for B cell-dependent humoral responses. To investigate the functions of Tfh cells in our EAMG model, Tfh cells were co-cultured with B cells. Briefly, CD4$^+$ T cells were isolated from both CFA

and EAMG rats and then each set of cells was stimulated by AChR (10 μg/mL) for 24 h *in vitro* to undergo AChR-specific Tfh cell activation. Higher levels of AChR-specific CD4$^+$CXCR5$^+$ICOS^{++} Tfh cell ratios were found in the EAMG rats than in the control rats (Fig. 5A–C). Then purified B cells isolated from EAMG rats were added into each T cell culture system for another 24 h. Data showed that the number of IgG2b-secreting B cells (Fig. 5D–F) and the level of anti-AChR antibodies in the supernatants (Fig. 5G) were increased in the co-cultures containing EAMG-derived Tfh cells. These results are consistent with the results shown in Fig. 2 that EAMG rats have much higher concentrations of anti-AChR IgGs in serum, implying a facilitating role of Tfh cells on AChR-specific B cell antibody secretion.

Expression of Bcl-6 in Lymphoid Organs

Bcl-6 is a crucial transcription factor in the differentiation of Tfh cells, and thus is regarded as a master transcription factor in Tfh cells [27]. Therefore, we used immunohistochemistry and immunofluorescence assays to detect Bcl-6 expression in lymphoid organs during the late stage of disease. There were a large number of Bcl-6-positive cells in the EAMG lymph node tissue (Fig. 6B), while they were
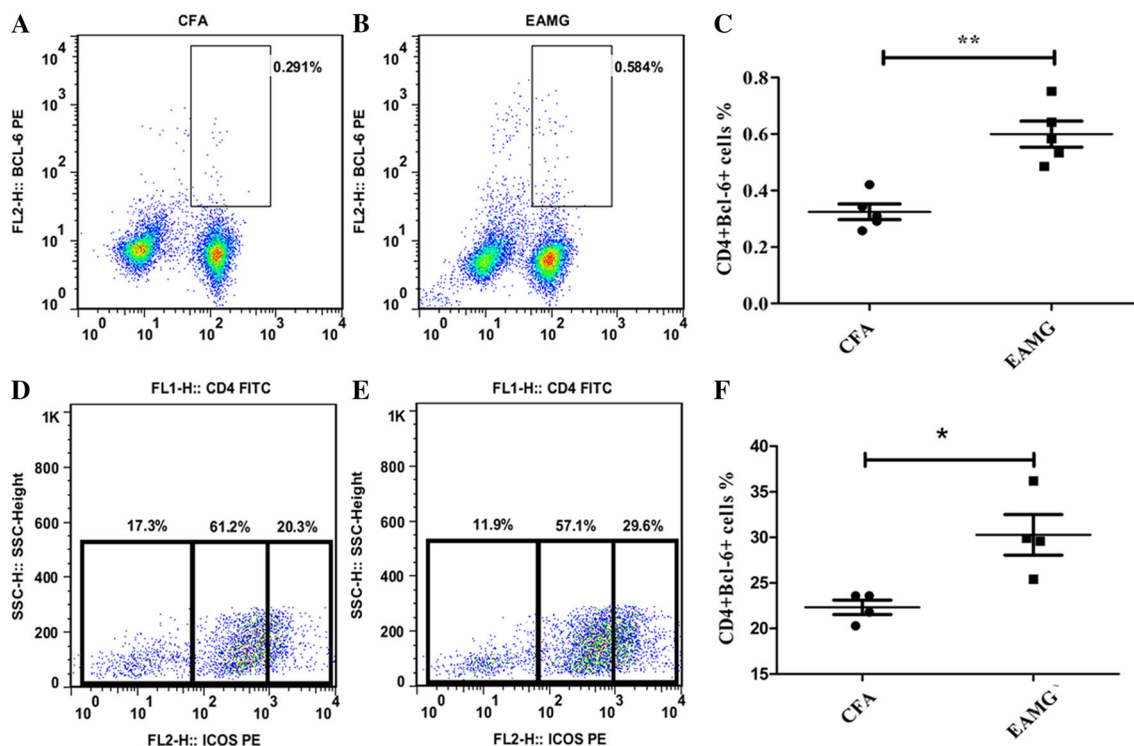

Fig. 4 Tfh profile during EAMG development. Tfh expression in lymphoid tissues at a late stage of disease measured by flow cytometry. CD4$^+$Bcl-6$^+$ cells (**A**, **B**) and CD4$^+$CXCR5$^+$ICOS^{++} cells (**D**, **E**) detected by staining. **C**, **F** Percentages of CD4$^+$Bcl-6$^+$ T cells in **A** and **B**, and CD4$^+$CXCR5$^+$ICOS^{++} cells (the left populations in **D** and **E**), respectively. Mean ± SD from three independent experiments with 4 to 5 rats per condition per experiment (*$P < 0.05$, **$P < 0.01$).

Fig. 5 Elevated anti-AChR IgG levels in B cells co-cultured with Tfh cells. **A**, **B** The ratio of AChR-specific CD4$^+$CXCR5$^+$ ICOS^{++} Tfh cells in the EAMG samples was 3–4-fold that in the CFA samples as detected by flow cytometry (**C**; ***$P < 0.001$). More IgG2b-secreting B cells were found in EAMG rats (**E**) than in CFA rats (**D**, **F**; ***$P < 0.001$) after 24 h of co-incubation with AChR-stimulated Tfh cells and the level of anti-AChR antibodies in the supernatant (**G**; **$P < 0.01$) was also elevated in the EAMG group. Data are from two independent experiments with 4–6 rats per condition per experiment and are expressed as the mean ± SD (**$P < 0.01$).
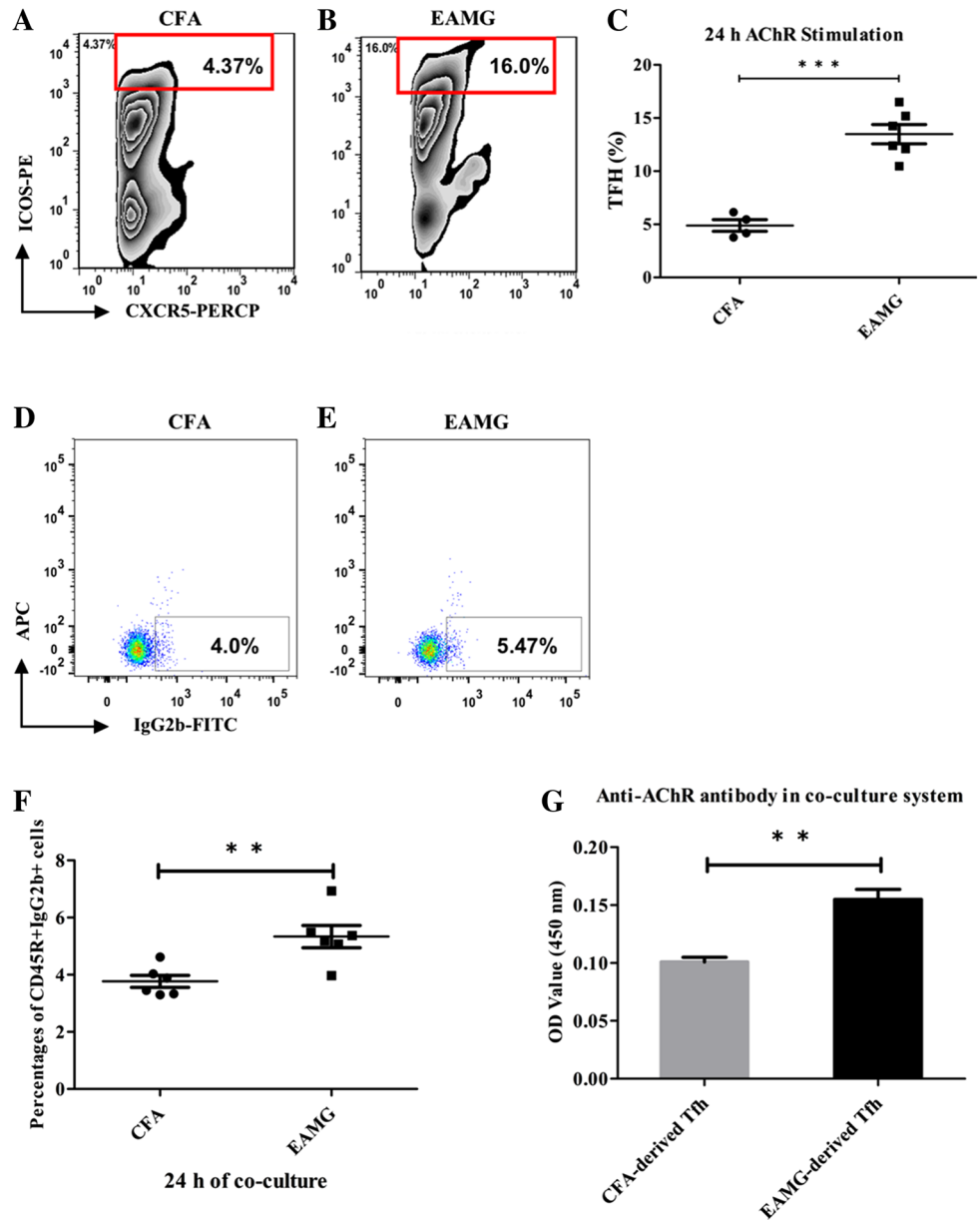
rarely seen in the CFA rats (Fig. 6A). Since both B cells and Tfh cells express Bcl-6, immunofluorescence assays were used to identify Bcl-6 expression by Tfh cells in lymphoid organs by double staining with antibodies recognizing CD4 and Bcl-6 (Fig. 6C, D). In lymph node tissues resected from CFA rats, only a few CD4$^+$/Bcl-6$^+$ T cells were observed. In contrast, a substantial number of CD4$^+$/Bcl-6$^+$ T cells were observed in lymph node tissues resected from EAMG rats.

Purified CD4$^+$ T cells were also collected and the mRNA level of Bcl-6 was analyzed by semi-quantitative-PCR. No amplification was found for the non-AChR-specific T cells, while amplification occurred in the EAMG

T cells (Fig. 6E). Altogether, these data confirm that the Tfh cells contribute to EAMG.

GC Formation in Lymphoid Organs

GCs are located in secondary lymphoid organs and are critical for T cell-dependent humoral responses. B cell activation also occurs in GCs, and this process is assisted by antigen-specific T cells [28]. Staining for PNA was performed on day 10 (the early phase of the disease) and on day 37 (the late stage) after primary immunization to examine GC formation in the lymph organs of EAMG and CFA rats. A greater number of larger GCs formed in the
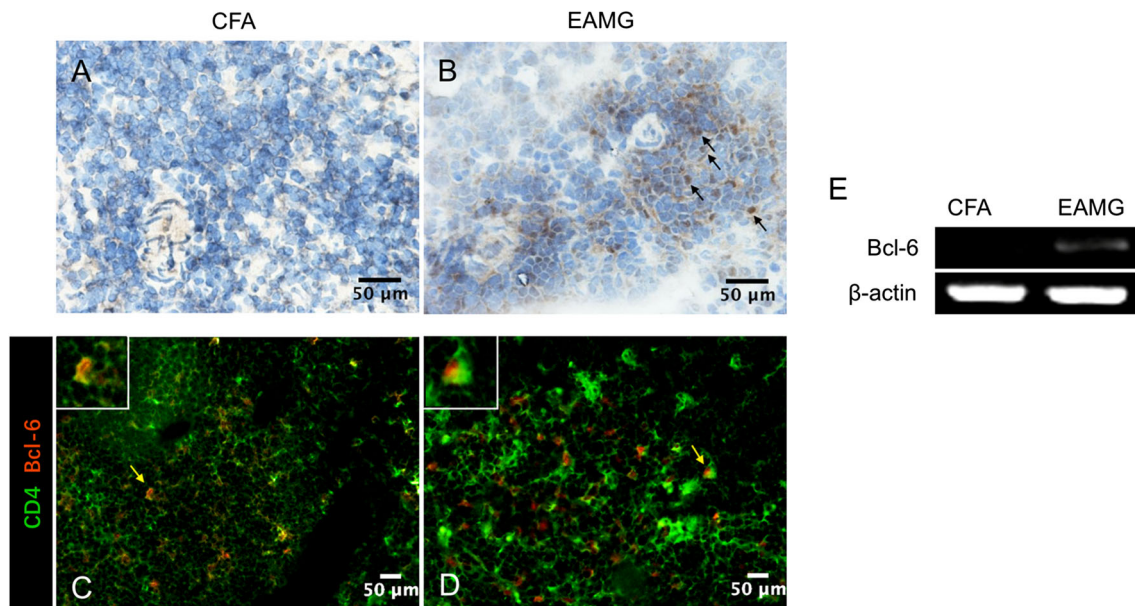
Fig. 6 Bcl-6 expression in lymph nodes. **A, B** Immunohistochemical staining was used to detect Bcl-6-positive cells in lymphoid tissues from CFA (**A**) and EAMG (**B**) rats (scale bars, 50 μm; arrows indicate positive cells). **C, D** Immunofluorescence assays were used to detect cells positively stained for CD4 (green) and Bcl-6 (red) (Tfh cells) in lymphoid tissue (scale bars, 50 μm; arrows indicate positive cells which are further magnified in the white boxes). **E** Bcl-6 and β-actin mRNA levels were assessed by semi-quantitative RT-PCR in CD4$^+$ T cells that were isolated and purified from lymph nodes from both groups. Data are from two independent experiments with 3–4 rats per condition per experiment.

lymph nodes of EAMG rats (Fig. 7B, D), while only a few PNA-positive GCs were observed in the lymph nodes of the CFA control rats (Fig. 7A, C).

Next, PNA-positive T cells and B cells were detected in lymph node tissue. The ratios of PNA-positive T cells and B cells were markedly higher in the EAMG tissue than in the CFA control tissue (Fig. 7E, F). Taken together, these results indicated that the humoral immune responses in EAMG rats are promoted by GC reactions in the context of an AChR-dependent antibody response.

Enhanced Cross-Talk Between T Cells and B Cells Via CD86

In adaptive immune responses, the cell surface molecules B7.1 (CD80), B7.2 (CD86), and ICOSL, which are expressed by antigen-presenting cells, interact with CD28 and ICOS molecules expressed by CD4$^+$ T cells. An interaction of CD86 and CD28 is necessary for B cell activation. However, in the context of viral infection [29], B cell-specific expression of CD86, but not CD80, is critical for the formation of Tfh cells. Moreover, there is a feedback loop, in which IL-21 produced by Tfh cells enhances the expression of CD86 [30] and this promotes the generation of Tfh cells [29, 31]. Here, we examined CD86 expression by B cells in our model by flow cytometry. The level of CD86 expressed by the AChR-specific B cells (CD45R$^+$ cells) collected from EAMG rats was nearly twice that of

the non-AChR-specific B cells collected from CFA rats (Fig. 8) at both early and late stages of disease. This result is consistent with the higher ratio of Tfh cells in the EAMG group than in the CFA group.

Discussion

The important role of B cells in the pathogenesis of MG is well established. However, CD4$^+$ T cells are also indispensable, based on their secretion of distinct cytokines and expression of several transcription factors that are needed for the production of antibodies by B cells [32, 33]. In addition, Tfh cells, rather than other helper T cells, are considered critical for the activation of B cells and B cell receptors, and for the formation of GCs. Hence, while Tfh cells have been associated with various autoimmune diseases, and abnormal expression of Tfh cells has been reported in MG patients, it remains unclear how and when Tfh cells are induced and how they may drive the progression of MG [18]. By using an EAMG rat model, we provided evidence that an aberrant increase in the number of pre-Tfh cells occurs during the early stage of EAMG, and this facilitates the formation of GCs and the secretion of antibodies by B cells. We further found that an AChR-specific induction of Tfh cells occurred during the late stage of EAMG, concomitant with the relatively clear pathological AChR loss in muscle.
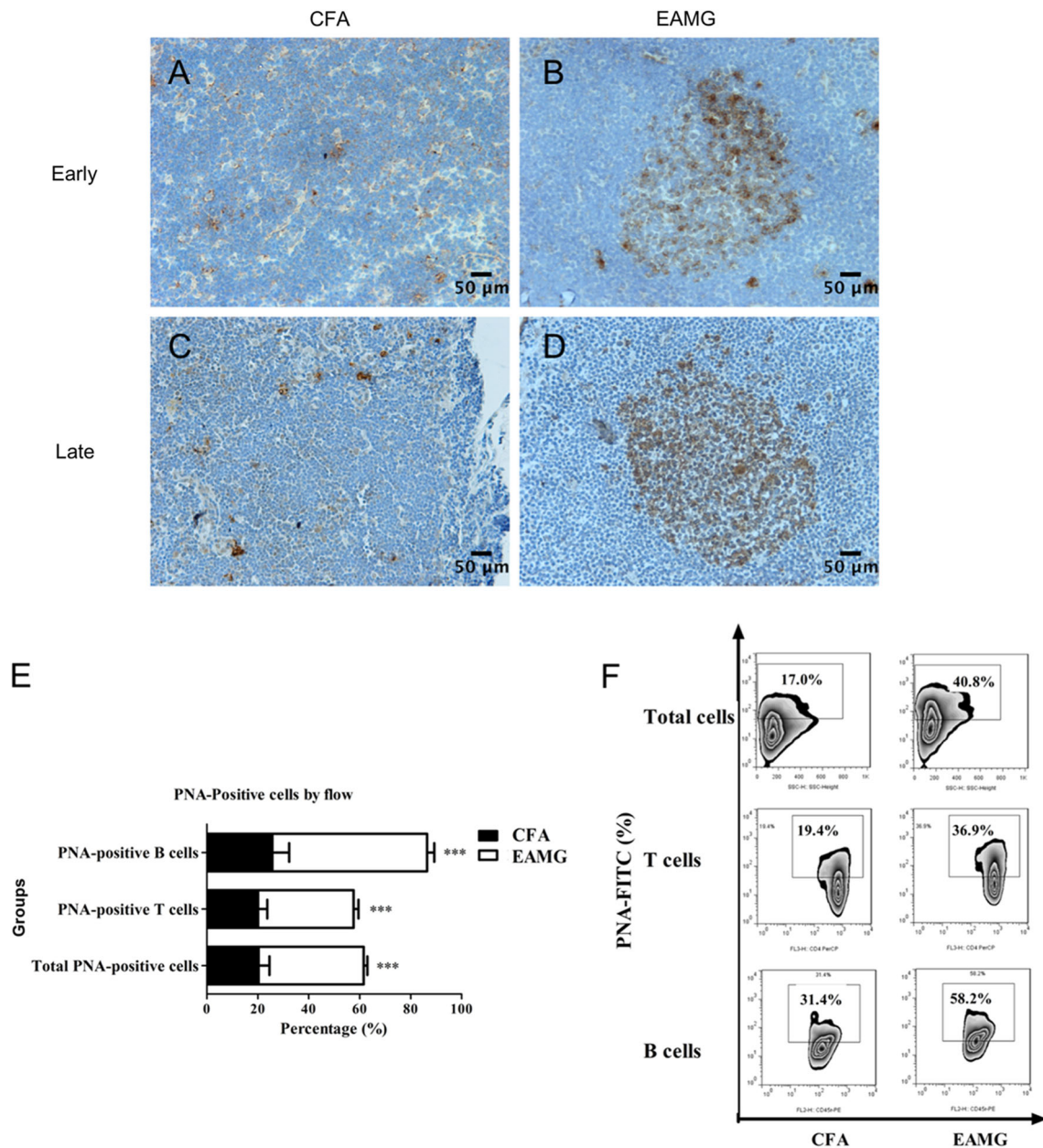
Fig. 7 GC response. Lymph nodes were resected during the early and late stages of disease and then stained with PNA to identify GCs. **A–D** Representative images showing the differences in GC size between the two groups (scale bars, 50 μm). **E, F** T cells, B cells, and total lymphocytes were isolated from lymph node tissue during the late stage of disease, stained for PNA, and analyzed by flow cytometry. The ratios of PNA-positive cells are expressed as the mean ± SD (**E, F**; ***$P < 0.001$). Data are from three independent experiments with 3–4 rats per condition per experiment.

Mice lacking Tfh cells are characterized by an absence of class-switched antibodies and abnormal GC development [34, 35], demonstrating a significant role for Tfh cells in B cell-mediated immune responses. Elevated levels of circulating Tfh cells have also been reported in patients with systemic lupus erythematosus [13], rheumatoidarthritis [14], and in some MG patients [18]. Meanwhile, no changes in the numbers of Tfh cells have been reported in corresponding controls, indicating that a positive

relationship exists between Tfh cells and the progression of antibody-mediated autoimmune diseases. Consequently, the role and functions of Tfh cells in MG are of great interest.

In the present study, a population of pre-Tfh cells was detected during the early stage of EAMG, despite the phenotypic immaturity of the rat model examined. In addition, AChR-specific autoantibodies were detected in the serum of AChR-immunized mice. As shown in Fig. 3,
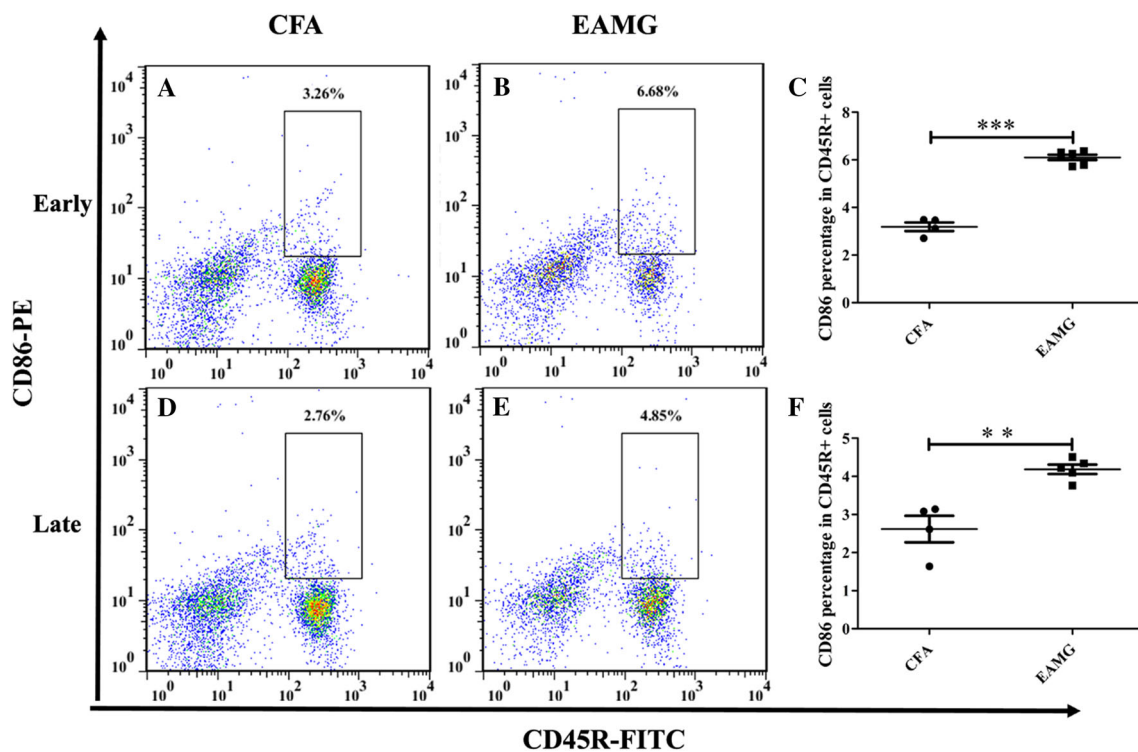
Fig. 8 CD86 expression on B cells. CD45R$^+$ B cells were isolated from lymph node tissue that was resected from EAMG (**B**, **E**) and CFA (**A**, **D**) rats and analyzed by flow cytometry during the early and late stages of disease. Compared with CFA group, the percentages of CD45R$^+$CD86$^+$ cells in EAMG group were statistically elevated at both early and late time points (**C**, **F**; **P < 0.01, ***P < 0.001). Data are shown as mean ± SD from two independent experiments with 4–5 rats per condition per experiment.

abnormal presentation of pre-Tfh cells was found 10 days after the initiation of EAMG, and the level of these cells continued to increase in parallel with EAMG progression (Fig. 4) and was accompanied by the development of hyperactive GCs in lymph nodes (Fig. 7). During the late stage of disease, a marked reduction in the number of clustered AChRs resulted in weaker and elongated α-BTX staining, implying an antibody-mediated attack on AChRs (Fig. 2C–E). When severe loss of AChRs was achieved with the assistance of Tfh cells, high levels of AChR-autoantibodies in serum (Fig. 2A, B) and high proportions of CD4$^+$Bcl-6$^+$ and CD4$^+$CXCR5$^+$ICOS^{high} Tfh cells were found (Fig. 4A–F). Co-culture assays of Tfh cells and B cells further demonstrated that secretion of anti-AChR antibodies by B cells was promoted by AChR-specific Tfh cells (Fig. 5). These results confirmed that Tfh cells are an important helper T cell population for B cell-dependent humoral responses and they also provide support for the finding that EAMG rats have higher concentrations of anti-AChR IgGs in the serum (Fig. 2), consistent with a role for Tfh cells in promoting the secretion of antibodies by AChR-specific B cells (Fig. 5).

Bcl-6 has been characterized as a key transcription factor in Tfh cells, mainly due to its role in allowing Tfh cells to promote antibody production by B cells [36, 37].

Correspondingly, T cells deficient in Bcl-6 fail to differentiate into Tfh cells and they do not maintain GCs [36]. In contrast, overexpression of Bcl-6 in CD4$^+$ T cells leads to an increase in the expression of cell surface molecules on Tfh cells, including PD-1, CXCR4, and CXCR5 [34]. When we used immunohistochemistry and immunofluorescence assays to confirm the presence and localization of Tfh cells in our EAMG model, we observed an aggregation of CD4$^+$Bcl-6$^+$ Tfh cells in the lymph nodes of EAMG rats during the late stage of disease (Figs. 4A–C and 6). After their initial contact with antigen, antigen-specific B cells have to compete for T cell help by presenting a cognate antigen to the T cells in order to be selected to enter a GC [38]. Tfh cells are also a limiting factor in the selection of B cells which will undergo affinity maturation of their B cell receptor genes and differentiate into longer-lived plasma or memory cells in GCs [39]. The lymph nodes of EAMG rats contained enlarged GCs (Fig. 7B, D) and a greater number of PNA$^+$ T/B cells (Fig. 7E, F), implying a function for Tfh cells in GCs.

Overall, the present results demonstrate that AChR-specific pre-Tfh and Tfh cells trigger the formation of GCs and the production of AChR-specific antibodies in the EAMG rat model and this induces muscle weakness and contributes to the development and progression of EAMG.

It remains for these insights to be confirmed in clinical cases.

Conflict of interest None of the authors have any conflict of interest to report.

References

1. Jayam Trouth A, Dabi A, Solieman N, Kurukumbi M, Kalyanam J. Myasthenia gravis: a review. Autoimmune Dis 2012, 2012: 874680.
2. Vincent A. Unravelling the pathogenesis of myasthenia gravis. Nat Rev Immunol 2002, 2: 797–804.
3. Shi QG, Wang ZH, Ma XW, Zhang DQ, Yang CS, Shi FD, *et al.* Clinical significance of detection of antibodies to fetal and adult acetylcholine receptors in myasthenia gravis. Neurosci Bull 2012, 28: 469–474.
4. Victora GD, Schwickert TA, Fooksman DR, Kamphorst AO, Meyer-Hermann M, Dustin ML, *et al.* Germinal center dynamics revealed by multiphoton microscopy with a photoactivatable fluorescent reporter. Cell 2010, 143: 592–605.
5. Nieuwenhuis P, Opstelten D. Functional anatomy of germinal centers. Am J Anat 1984, 170: 421–435.
6. Vinuesa CG, Linterman MA, Yu D, MacLennan ICM. Follicular helper T cells. Annu Rev Immunol 2016, 34: 335–368.
7. Crotty S. A brief history of T cell help to B cells. Nat Rev Immunol 2015, 15: 185.
8. Schaerli P, Willimann K, Lang AB, Lipp M, Loetscher P, Moser B. CXC chemokine receptor 5 expression defines follicular homing T cells with B cell helper function. J Exp Med 2000, 192: 1553–1562.
9. Breitfeld D, Ohl L, Kremmer E, Ellwart J, Sallusto F, Lipp M, *et al.* Follicular B helper T cells express CXC chemokine receptor 5, localize to B cell follicles, and support immunoglobulin production. J Exp Med 2000, 192: 1545–1552.
10. Nutt SL, Hodgkin PD, Tarlinton DM, Corcoran LM. The generation of antibody-secreting plasma cells. Nat Rev Immunol 2015, 15: 160–171.
11. Ise W, Fujii K, Shiroguchi K, Ito A, Kometani K, Takeda K, *et al.* T follicular helper cell-germinal center B cell interaction strength regulates entry into plasma cell or recycling germinal center cell fate. Immunity 2018, 48: 702–715.e4.
12. Bossaller L, Burger J, Draeger R, Grimbacher B, Knoth R, Plebani A, *et al.* ICOS deficiency is associated with a severe reduction of CXCR5+CD4 germinal center Th cells. J Immunol Baltim Md 2006, 177: 4927–4932.
13. Simpson N, Gatenby PA, Wilson A, Malik S, Fulcher DA, Tangye SG, *et al.* Expansion of circulating T cells resembling follicular helper T cells is a fixed phenotype that identifies a subset of severe systemic lupus erythematosus. Arthritis Rheum 2010, 62: 234–244.
14. Liu R, Wu Q, Su D, Che N, Chen H, Geng L, *et al.* A regulatory effect of IL-21 on T follicular helper-like cell and B cell in rheumatoid arthritis. Arthritis Res Ther 2012, 14: R255.
15. Schmitt N. Role of T follicular helper cells in multiple sclerosis. J Nat Sci 2015, 1: e139.
16. Fan X, Jiang Y, Han J, Liu J, Wei Y, Jiang X, *et al.* Circulating memory t follicular helper cells in patients with neuromyelitis optica/neuromyelitis optica spectrum disorders. Mediators Inflamm 2016, 2016: 3678152.
17. Wen Y, Yang B, Lu J, Zhang J, Yang H, Li J. Imbalance of circulating CD4(+)CXCR5(+)FOXP3(+) Tfr-like cells and CD4(+)CXCR5(+)FOXP3(-) Tfh-like cells in myasthenia gravis. Neurosci Lett 2016, 630: 176–182.
18. Zhang M, Zhou Y, Guo J, Li H, Tian F, Gong L, *et al.* Thymic TFH cells involved in the pathogenesis of myasthenia gravis with thymoma. Exp Neurol 2014, 254: 200–205.
19. Schmitt N, Bentebibel SE, Ueno H. Phenotype and functions of memory Tfh cells in human blood. Trends Immunol 2014, 35: 436–442.
20. Wu B, Goluszko E, Huda R, Tüzün E, Christadoss P. Experimental autoimmune myasthenia gravis in the mouse. Curr Protoc Immunol 2013. https://doi.org/10.1002/0471142735.im1508s100.
21. Hamaoka T, Katz DH, Benacerraf B. Hapten-specific IgE antibody responses in mice. J Exp Med 1973, 138: 538–556.
22. Abbas AK, Murphy KM, Sher A. Functional diversity of helper T lymphocytes. Nature 1996, 383: 787–793.
23. Xie X, Mu L, Yao X, Li N, Sun B, Li Y, *et al.* ATRA alters humoral responses associated with amelioration of EAMG symptoms by balancing Tfh/Tfr helper cell profiles. Clin Immunol Orlando Fla 2013, 148: 162–176.
24. Mantegazza R, Cordiglieri C, Consonni A, Baggi F. Animal models of myasthenia gravis: utility and limitations. Int J Gen Med 2016, 9: 53–64.
25. Losen M, Martinez-Martinez P, Molenaar PC, Lazaridis K, Tzartos S, Brenner T, *et al.* Standardization of the experimental autoimmune myasthenia gravis (EAMG) model by immunization of rats with *Torpedo californica* acetylcholine receptors—recommendations for methods and experimental designs. Exp Neurol 2015, 270: 18–28.
26. Gao B, Kong Q, Zhang Y, Yun C, Dent SYR, Song J, *et al.* The histone acetyltransferase Gcn5 positively regulates T cell activation. J Immunol 1950 2017, 198: 3927–3938.
27. Chtanova T, Tangye SG, Newton R, Frank N, Hodge MR, Rolph MS, *et al.* T follicular helper cells express a distinctive transcriptional profile, reflecting their role as non-Th1/Th2 effector cells that provide help for B cells. J Immunol 2004, 173: 68–78.
28. Domeier PP, Schell SL, Rahman ZSM. Spontaneous germinal centers and autoimmunity. Autoimmunity 2017, 50: 4–18.
29. Salek-Ardakani S, Choi YS, Rafii-El-Idrissi Benhnia M, Flynn R, Arens R, Shoenberger S, *et al.* B cell-specific expression of B7-2 is required for follicular Th cell function in response to vaccinia virus. J Immunol 2011, 186: 5294–5303.
30. Attridge K, Kenefeck R, Wardzinski L, Qureshi OS, Wang CJ, Manzotti C, *et al.* IL-21 promotes CD4 T cell responses by phosphatidylinositol 3-kinase-dependent upregulation of CD86 on B cells. J Immunol Author Choice 2014, 192: 2195–2201.
31. Vogelzang A, McGuire HM, Yu D, Sprent J, Mackay CR, King C. A fundamental role for interleukin-21 in the generation of T follicular helper cells. Immunity 2008, 29: 127–137.
32. Masi A, Glozier N, Dale R, Guastella AJ. The immune system, cytokines, and biomarkers in autism spectrum disorder. Neurosci Bull 2017, 33: 194–204.
33. Jayam Trouth A, Dabi A, Solieman N, Kurukumbi M, Kalyanam J. Myasthenia gravis: a review. Autoimmune Dis 2012, 2012: 874680.

518

Neurosci. Bull. June, 2019, 35(3):507–518

34. Arnold CN, Campbell DJ, Lipp M, Butcher EC. The germinal center response is impaired in the absence of T cell-expressed CXCR5. Eur J Immunol 2007, 37: 100–109.

35. Kim HJ, Verbinnen B, Tang X, Lu L, Cantor H. Inhibition of follicular T-helper cells by CD8(+) regulatory T cells is essential for self tolerance. Nature 2010, 467: 328–332.

36. Johnston RJ, Poholek AC, DiToro D, Yusuf I, Eto D, Barnett B, *et al.* Bcl6 and Blimp-1 are reciprocal and antagonistic regulators of T follicular helper cell differentiation. Science 2009, 325: 1006–1010.

37. Yu D, Rao S, Tsai LM, Lee SK, He Y, Sutcliffe EL, *et al.* The transcriptional repressor Bcl-6 directs T follicular helper cell lineage commitment. Immunity 2009, 31: 457–468.

38. Schwickert TA, Victora GD, Fooksman DR, Kamphorst AO, Mugnier MR, Gitlin AD, *et al.* A dynamic T cell–limited checkpoint regulates affinity-dependent B cell entry into the germinal center. J Exp Med 2011, 208: 1243–1252.

39. Victora GD, Nussenzweig MC. Germinal centers. Annu Rev Immunol 2012, 30: 429–457.